JOURNAL PRE-PROOF

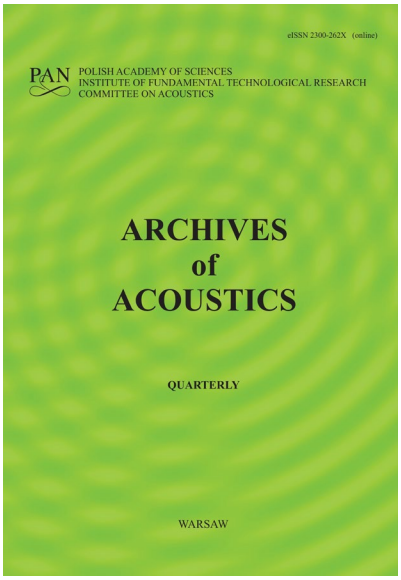

Title: Study on the Physical Mechanism of Rhodamine B Degradation by Ultrasonic Cavitation Effect

Author(s): Jiayuan Wang, Yan Ma

DOI: https://doi.org/10.24423/archacoust.2026.4299

Journal: *Archives of Acoustics*

ISSN: 0137-5075, e-ISSN: 2300-262X

Publication status: In press

Received: 2025-08-13

Revised: 2026-02-20

Accepted: 2026-07-13

Published pre-proof: 2026-07-27

Please cite this article as:

Wang J., Ma Y. (2026), Study on the Physical Mechanism of Rhodamine B Degradation by Ultrasonic Cavitation Effect, *Archives of Acoustics*, https://doi.org/10.24423/archacoust.2026.4299

Study on the Physical Mechanism of Rhodamine B Degradation by Ultrasonic Cavitation Effect

Jiayuan Wang, Yan Ma*✉

College of Physics and Electronic Information Engineering, Ning Xia Normal University, Guyuan, China

Corresponding author email: manyan_2050@163.com

The growing environmental challenge posed by textile effluents has driven the search for effective and sustainable treatment technologies. Ultrasonic degradation has emerged as a promising approach due to its ability to break down organic pollutants without introducing secondary contamination. However, the underlying physical mechanisms remain insufficiently understood, limiting the optimization of energy efficiency in practical applications. To address this gap, this study employs Rhodamine B (Rh B) as a model pollutant to investigate the fundamental principles governing ultrasonic degradation through a multi-faceted approach. First, the cavitation activity of the acoustic field under varying ultrasonic parameters is quantitatively evaluated using potassium iodide (KI) dosimetry. Second, systematic experiments are conducted to examine the synergistic effects of acoustic field intensity, sonication time, ultrasonic frequency, and power on the degradation efficiency of Rh B. Third, theoretical and numerical simulations are performed to analyze the nonlinear oscillation behavior of a single cavitation bubble and its influencing factors, thereby elucidating the physical mechanisms driving degradation. The experimental results reveal that bubble oscillation-induced cavitation generates localized high temperatures and pressures, which facilitate the cleavage of molecular bonds in Rh B. The degradation rate exhibits a positive correlation with both cavitation activity and acoustic field intensity, synergistically modulated by the operational parameters. A key novelty of this work lies in establishing an explicit correlation between parametric experimental results and detailed bubble dynamics simulations, providing mechanistic insights that extend beyond phenomenological observation. Together, these findings offer a theoretical and experimental foundation for optimizing energy efficiency in the ultrasonic degradation of organic pollutants.

Keywords: Ultrasonic cavitation, Rhodamine B, Cavitation activity, Acoustic field intensity, Bubble dynamics

1. Introduction

In recent years, with the development of the textile dyeing and printing industry, a large amount of printing and dyeing wastewater has been discharged into the environment, which is characterized by a high color intensity, difficult biodegradability and high biological toxicity (Hao O. J. *et al*., 2000; Holkar C.R. *et al*., 2016; Liu Z. C., *et al*., 2022). It is difficult to efficiently degrade the printing and dyeing wastewater by the traditional wastewater treatment technology. As a result, achieving environmentally friendly treatment of textile effluents while preventing secondary pollution has become a critical research focus (Sadeghi M., Zarshenas P., 2024; Liu S. *et al*., 2025). Among emerging treatment technologies, the ultrasonic degradation of the organic pollutants in water, especially refractory organic compounds, has shown several significant advantages including safety, environmental friendliness, without creating a secondary pollution, which exhibits the substantial potential for the future development (Kashyap N. *et al*., 2020; Alfonso-Muniozguren P. *et al*., 2021;Chen H. *et al*., 2024).

The fundamental principle of ultrasonic degradation of organic pollutants seems to be due to the cavitation effect produced by the ultrasonic waves. When ultrasonic waves propagate through the liquid can form an acoustic pressure field. Under the alternating positive and negative effects of acoustic pressure, countless tiny bubbles are generated in the liquid where they continuously grow and collapse with the influence of acoustic waves (Kanthale P. *et al*., 2008; Wei H. *et al*. 2024; Wang B. et al., 2024). The collapse of cavitation bubbles may generate a localized high temperature, high pressure, and shock waves, providing extreme physicochemical conditions for the chemical reaction, which may cause the decomposition of water vapor inside the bubbles into H· and OH· radicals. The resulting OH· radicals consequently oxidize Rh B, leading to its degradation (Merouani S. *et al*., 2010; Ma Y. *et al*., 2012; Chen X. *et al*., 2016).

Although ultrasonic degradation of organic pollutants holds promise, the underlying degradation mechanisms remain insufficiently understood and warrant more systematic and mechanistic investigation. Specifically, how to tune acoustic field parameters—such as frequency and power—to maximize energy release during bubble collapse for efficient degradation remains unclear. Many studies focus either on macroscopic degradation experiments or on theoretical bubble simulations—few tightly couple both to uncover mechanisms. To address this gap, we employed the Rh B solution as a model pollutant and conducted research through the following aspect: (1) to quantify cavitation activity and the Rh B degradation efficiency across acoustic parameters; (2) to simulate nonlinear oscillation behavior of the

bubble; and (3) to elucidate the physical mechanisms underlying ultrasonic degradation of organic pollutants, thereby providing theoretical and experimental support for the degradation of printing and dyeing wastewater.

2. Materials and Methods

2.1. Materials and Experimental Setup

Rhodamine B (Rh B, $C_{28}H_{31}ClN_2O_3$, analytical grade) was used to prepare simulated printing and dyeing wastewater. Potassium iodide (KI, analytical grade) was used for cavitation activity measurements. All chemicals were purchased from Lanzhou Honghao Instrument & Equipment Co., Ltd. All solutions were prepared using deionized water.

The experiment employed a KQ-300VDE triple-frequency digital ultrasonic cleaner (Kunshan Ultrasonic Instrument Co., Ltd.) as the core ultrasonic irradiation source, with an adjustable output power ranging from 120 W to 300 W and three fixed operating frequencies of 45 kHz, 80 kHz, and 100 kHz. Reactions were conducted in a cylindrical glass beaker with a diameter of 8 cm and a volume of 500 mL, with 350 mL of solution added for each experiment.

Figure 1 Schematic diagram of the experimental setup (Inner tank dimensions:300×240×150 mm.)

The acoustic field intensity was measured using an acoustic intensity meter (Suzhou Shengbo Ultrasonic Technology Co., Ltd.), and the acoustic intensity probe was positioned 2 cm below the liquid surface at the center of the beaker to obtain the spatially averaged acoustic intensity at that plane. The concentration of RhB was determined using an ultraviolet-visible spectrophotometer (Shanghai Meipuda Instrument Co., Ltd.), with absorbance recorded at the characteristic wavelength of 523 nm and quantified based on a standard calibration curve. Precise weighing of samples was performed using an ES-E320A analytical balance (Tianjin De'ante Sensing Technology Co., Ltd.). The THQZL-1 Surface Tension Measuring Instrument (Zhejiang Tianhuang Technology Experiment Co., Ltd.) was employed to determine

the surface tension of the test solution. A complete schematic diagram of the experimental setup is shown in Figure 1.

2.2. Experimental Procedures

2.2.1. Measurement of cavitation activity in the acoustic field

Cavitation activity was semi-quantitatively assessed using the standard iodometric dosimetry method (Tatake, Pandit, 2002; Gogate *et al*., 2001). The principle is that the extremely high temperature and high pressure generated when cavitation bubbles collapse are sufficient to cause the decomposition of water vapor within the bubbles and generate hydroxyl radicals (OH·), which subsequently recombine to form hydrogen peroxide (H_2O_2). H_2O_2 then oxidizes iodide ions (I^-) in solution to iodine (I_2), which further complexes with excess I^- to form triiodide ions (I_3^-), which exhibit a characteristic absorption peak at 352 nm. The following reaction occurs when the KI solution is irradiated with the ultrasound (Xu W. *et al*.,2006; Li W., 2023):

$$H_2O \rightarrow H^+ + OH^- \quad (1)$$

$$2 \cdot OH^- \rightarrow H_2O_2 \quad (2)$$

$$H_2O_2 + 2KI \rightarrow 2KOH + I_2 \quad (3)$$

$$I^- + I_2 \rightleftharpoons I_3^- \quad (4)$$

The above equation indicates that the amount of I_3^- generated is equivalent to the amount of H_2O_2.Thus, measuring the concentration of I_3^- indirectly reflects the total amount of chemically active species generated by acoustic cavitation. A 0.1 mol/L KI solution was sonicated under specific frequency and power conditions for 60 minutes. Samples were taken at 10-minute intervals, and through the ultraviolet spectrophotometer, measuring the concentration of the KI solution at a wavelength of 352 nm can indirectly determine the cavitation activity of the acoustic field. Each experiment was performed in triplicate, and the average value is reported.

2.2.2. Ultrasonic Degradation of Rh B and Acoustic Intensity Measurement

Accurately weigh 50 mg of Rh B powder and transfer it into a beaker. Dissolve it with a small amount of water, then transfer it to a 500 mL volumetric flask. Dilute the mark with water to prepare a 0.1 g/L standard solution. Take 0 mL, 5 mL, 10 mL, 15 mL, 20 mL, and 25 mL aliquots of the prepared standard solution and transfer them into separate 250 mL volumetric flasks. Dilute each to the mark with water to prepare Rh B solutions with concentrations of 0 mg/L, 2 mg/L, 4 mg/L, 6 mg/L, 8 mg/L, and 10 mg/L respectively.

Samples of the Rh B solution at different concentrations are taken, and their absorbance is measured at a wavelength of 523 nm using an ultraviolet spectrophotometer. The standard curve is determined as C=14.0124×A+0.0188 and a correlation coefficient of 0.999913.

For degradation experiments, a 350 mL volume of 10 mg/L Rh B solution was sonicated under various conditions. Samples were taken at 10-minute intervals, and the Rh B concentration was determined using the standard curve. The degradation efficiency was calculated accordingly.

Acoustic field intensity (I, in W/cm^2) was measured directly using the sound intensity meter mentioned above. The probe was scanned within the reaction solution, and the reported value represents a spatial average.

2.3. Numerical Simulation Methods

2.3.1. Fluid Dynamics Simulation

To investigate the physical mechanisms of the ultrasonic degradation of Rh B, we simulated the evolution of a single bubble within the solution under the ultrasonic driving frequencies of 45 kHz, 80 kHz, and 100 kHz.

The motion of the bubble in a liquid medium constitutes a gas-liquid two phase flow problem. The finite element simulation model of the bubble in the fluid environment is constructed based on the COMSOL software environment. The evolution process of a single cavitation bubble in Rh B solution under the ultrasonic is simulated, which using the fluid dynamics control equation and the dynamic mesh model. The acoustic field distribution is calculated using the acoustic module, while the liquid flow is simulated with the laminar flow module, both satisfying the continuity equation and the Navier-Stokes equation:

$$\nabla \cdot u = 0 \tag{5}$$

$$\rho\left(\frac{\partial u}{\partial t} + (u \cdot \nabla)u\right) + \nabla \cdot (-pI + \mu(\nabla u + \nabla u^T)) = 0 \tag{6}$$

Where u and p respectively denote the flow velocity and pressure of the liquid, ρ denote the density of the liquid. I is the second-order unit tensor (the 3×3 identity matrix in three-dimensional space), and the term $\nabla \cdot (-pI)$ represents the pressure gradient force acting on a fluid element. The printing and dyeing wastewater is simulated using a Rh B solution.

2.3.2. Bubble Dynamics Simulation

To further explore the influencing factors of the ultrasonic degradation of Rh B, we studied the dynamic equation of a single bubble in Rh B solution. The cavitation effect under the influence of the ultrasonic in Rh B solution and its influencing factors are investigated using MATLAB software to numerically solve the bubble dynamics equation with the fourth-order Runge-kuta method.

The dynamic behavior of a bubble under the influence of ultrasonic waves is governed by the Herring-Trilling equation (Chen, 2014).

$$\left(1-\frac{\dot{R}}{c}\right)R\ddot{R}+\frac{3}{2}\dot{R}^2\left(1-\frac{\dot{R}}{3c}\right)=\frac{1}{\rho}\left(1+\frac{\dot{R}}{c}\right)P_s+\frac{R}{\rho c}\frac{\mathrm{d}}{\mathrm{d}t}P_s \tag{7}$$

In Eq. (7), where R_0 represents the initial radius of the bubble, R denotes the radius of the bubble at a given moment, and the point above R represents the derivative of time, and c denotes the propagation speed of the acoustic wave in the liquid, and ρ respectively denote the flow velocity and pressure of the liquid,.

$$P_s=P_g-\frac{2\sigma}{R}-4\mu\frac{\dot{R}}{R}-P_d\cos(2\pi ft)-P_0 \tag{8}$$

where σ is the surface tension coefficient of the liquid, μ is the viscosity coefficient of the liquid, P_d is the amplitude of the driving acoustic pressure, P_0 is the static pressure of the liquid, and f is the driving frequency of the acoustic fields. Assuming that the bubble undergoes adiabatic compression during its oscillatory motion, the internal pressure of the bubble P_g can be simply expressed based on the equation of state as:

$$P_g=(P_0+\frac{2\sigma}{R_0})(\frac{R_0}{R})^{3\gamma} \tag{9}$$

where γ represents the gas polytropic index, and the temperature inside the bubble T_g is given by:

$$T_g=T_0\left(\frac{R_0}{R}\right)^{3\gamma-3} \tag{10}$$

where T_0 is the ambient temperature of the bubble, and the Mach number M on the gas side can be expressed as:

$$M=\frac{|\dot{R}|}{C} \tag{11}$$

where C is the speed of acoustic in the gas, which can be expressed as (Métayer L. *et al*., 2016):

$$C=\sqrt{\gamma\frac{P_g}{\left(1-b\rho_g\right)}} \tag{12}$$

where b is the van der Waals excluded volume, and ρ_g denotes the density of the gas inside the bubble. The density, viscosity coefficient, and surface tension coefficient of the Rh B solution at a specific concentration are experimentally determined. The relevant parameters of the liquid and the bubble are as

follows: the initial radius of the bubble is 5 μm, the polytropic index of the gas inside the bubble is 1.4, and the ambient temperature surrounding the bubble is 296 K. Additionally, the static pressure of the liquid is 1.01×10^5 Pa, the speed of acoustic in the liquid is 1480 m/s, the liquid density is 984 kg/m^3, the viscosity coefficient is 1.01×10^{-3} Pa·s, and the surface tension coefficient is 0.032 N/m.

3. Measurements

3.1. Cavitation Activity under Different Acoustic Parameters

The ultrasonic driving frequency, sonication time, and ultrasonic power are important factors affecting the cavitation activity of the acoustic field. The KI solution is irradiated with ultrasound for 60 minutes. All concentration measurements are based on calibrated standard curves, with the concentration of I_3^- reported in mmol/L. The changes in the solution concentration are determined by ultraviolet spectrophotometer. The cavitation activity of the acoustic field is investigated at driving frequencies of 45 kHz, 80 kHz, and 100 kHz respectively, as well as the ultrasonic powers of 120 W, 180 W, and 240 W respectively. The results are shown in Figure 2 and Figure 3.

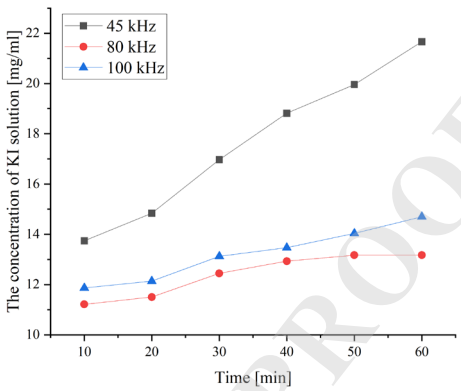

Figure 2 Effect of frequency on the concentration of KI solution.

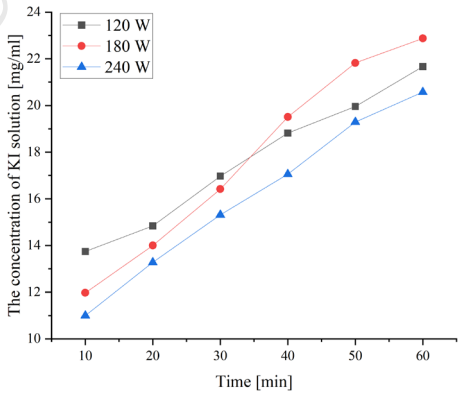

Figure 3 Effect of power on the concentration of KI solution.

The concentration of the KI solution measured at 352 nm after ultrasonic irradiation corresponds specifically to the concentration of triiodide ions (I_3^-) generated during cavitation. This is because I_3^- exhibits a characteristic absorption peak at 352 nm, whereas the original KI solution (containing I^- ions) has negligible absorbance at this wavelength. Therefore, the measured value directly represents the I_3^- concentration, which serves as a reliable indicator of cavitation activity. Figure 2 shows the concentration of KI solution continuously increases with the increasing sonication time at different ultrasonic frequencies, and the growth rate gradually slows down after 30 minutes. The experimental data shows that under the action of acoustic field with an ultrasonic driving frequency of 45 kHz. The growth rate of the concentration of I_3^- in the solution is significantly higher than under the action of acoustic fields with the

ultrasonic driving frequencies of 80 kHz and 100 kHz. It indicates that the cavitation activity in the acoustic field is higher under the action of a lower frequency acoustic field.

Figure 3 shows the concentration of KI solution continuously increases with the increasing sonication time at different ultrasonic power. The result indicate that when the ultrasonic power is 180 W, the growth rate of I_3^- concentration in the solution is the highest, which suggest that the cavitation activity of the acoustic field is the highest under these conditions.

3.2. Acoustic Field Intensity

The acoustic field intensity represents acoustic energy density introduced into the reaction liquid, which directly influences the magnitude of the acoustic cavitation effect. Thereby the acoustic field intensity can determine the intensity of cavitation bubble collapse and the subsequent physical and chemical phenomena.

The increase of the acoustic field intensity can promote both the formation and collapse of cavitation bubbles, as well as further enhance the efficiency of the Sono chemical reaction. Measuring the acoustic field intensity under various parametric conditions is crucial for understanding the underlying physical mechanisms involved in the ultrasonic degradation of Rh B.

Table 1 acoustic field intensity under different parameters.

Power（W） \ Frequency（kHz）	45	80	100
120	0.45 W/cm^2	0.25 W/cm^2	0.40 W/cm^2
180	0.54 W/cm^2	0.27 W/cm^2	0.44 W/cm^2
240	0.47 W/cm^2	0.25 W/cm^2	0.41 W/cm^2

Table 1 presents the spatially averaged acoustic field intensity measured under different combinations of frequency and power. It is important to note that the measured intensity depends not only on the generator's power setting and frequency but also on the transducer characteristics, reactor geometry, and resulting acoustic field distribution.

The results indicate that when the Rh B solution is subjected to an ultrasonic power of 180 W and a driving frequency of 45 kHz, the intensity of the acoustic field will reach the maximum.

3.3. Influencing factors of ultrasonic degradation of Rh B

3.3.1. The influence of the sonication time on the degradation rate of Rh B

The sonication time is a critical factor which influences the degradation efficiency of Rh B. During the degradation process, the cavitation effect generated by the acoustic field creates an extreme physical environment within the Rh B solution, which promotes the dissociation of water molecules into hydroxyl radicals. These reactive species subsequently combine to form hydrogen peroxide, which facilitates the oxidative degradation of pollutants.

Figure 4 shows that the degradation efficiency of Rh B increases with sonication time under the conditions of the acoustic field with a driving frequency of 45 kHz and a power of 120 W. The degradation rate is relatively rapid during the initial 30 minutes, after which the rate of improvement diminishes significantly. The experimental results indicate that the cavitation intensity is highest within the first 30 minutes, resulting in an increase in degradation efficiency. However, when the ultrasonic treatment continues, the concentration of bubbles in the solution decreases. This trend correlates with the observed slowdown in I_3^- production (Figure 2), potentially due to a reduction in the number of effective cavitation nuclei available over prolonged sonication or changes in solution conditions affecting cavitation thresholds, such as temperature rise and dissolved gas content. These results will lead to a reducing of the cavitation activity and a corresponding decline in hydrogen peroxide production. Consequently, the overall degradation efficiency also declines.

3.3.2. The influence of the ultrasonic driving frequency on the degradation rate of Rh B solution

The ultrasonic driving frequency is a critical parameter which influences the degradation efficiency of Rh B. As shown in Figure 4, the Rh B solution is irradiated with ultrasound for 60 minutes at different driving frequencies, during which the degradation rate is measured. The experimental result indicates that the degradation efficiency is the highest when the ultrasonic driving frequency is 45 kHz, while the degradation efficiency is the lowest when the driving frequency is 80 kHz. It's attributed to the frequency dependent characteristics of the cavitation activity and the intensity of the acoustic field. Specifically, under an ultrasonic driving frequency of 45 kHz, the cavitation activity and the intensity of the acoustic field reach maximum, leading to optimal energy coupling efficiency. This ranking aligns with the measured cavitation activity (Figure 2) and the general trend of acoustic intensity (Table 1), suggesting that the enhanced degradation at 45 kHz is driven by more intense cavitation.

3.3.3. The influence of ultrasonic power on the degradation rate of Rh B

Figure 5 shows that when the ultrasonic driving frequency is 45 kHz, the ultrasonic power may significantly influence the efficiency of the ultrasonic degradation of Rh B.

The experimental results indicate that within the initial 30 minutes, the degradation rate reaches its peak when the ultrasonic power is 120 W, and the degradation rate is lowest when the power is 240 W. However, beyond the 30 minutes mark, the degradation rate gradually increases and attains its maximum at 180 W, which is higher than those observed at 120 W and 240 W. This complex relationship suggests that while higher power generally delivers higher acoustic intensity (Table 1), there may be an optimal range. Excessive power might lead to the formation of a dense cloud of bubbles that shield the acoustic energy or cause other nonlinear effects that reduce the effective cavitation intensity for degradation.

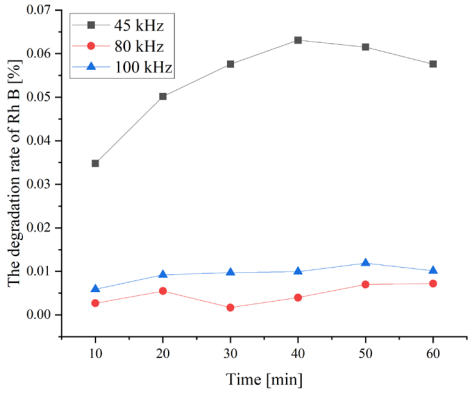

Figure 4 Effect of frequency on the degradation rate of Rh B.

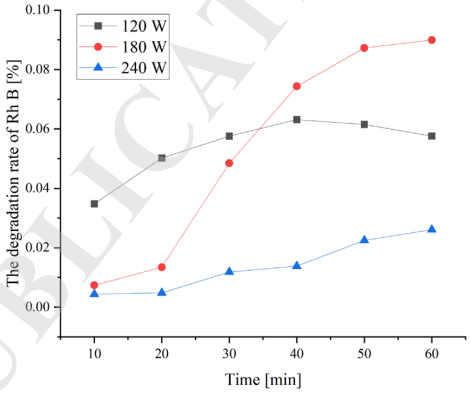

Figure 5 Effect of frequency on the degradation rate of Rh B.

4. Simulations

4.1. Investigation of nonlinear bubble oscillations in Rh B solution under ultrasonic excitation

The driving frequency of the acoustic field is a critical parameter which influences the nonlinear oscillation behavior of the bubble. In this study, we simulated the evolution process of a single bubble in the Rh B solution under the excitation of different acoustic driving frequencies, which is shown in Figure 6.

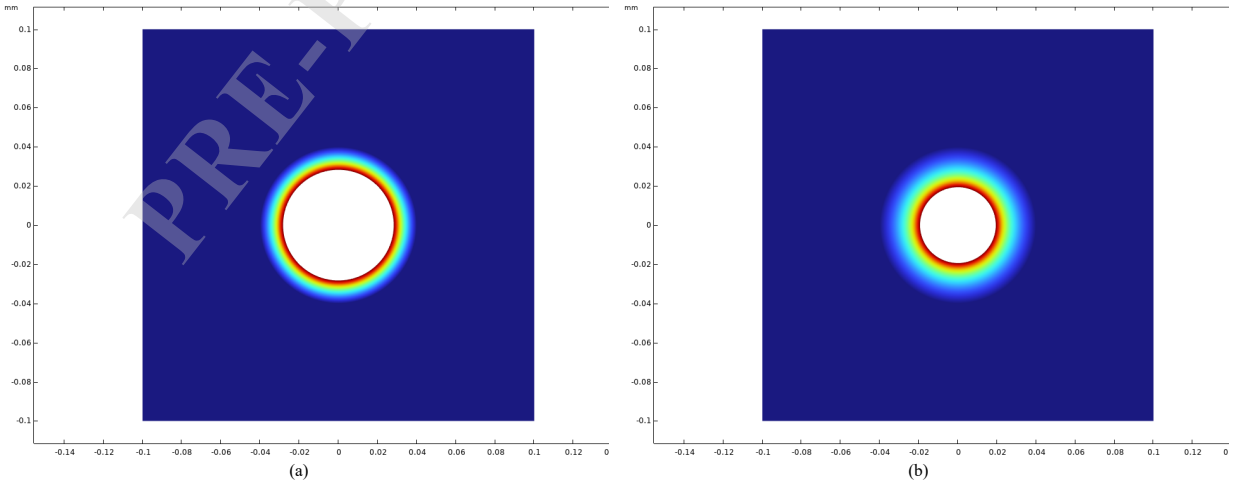

(a) (b)

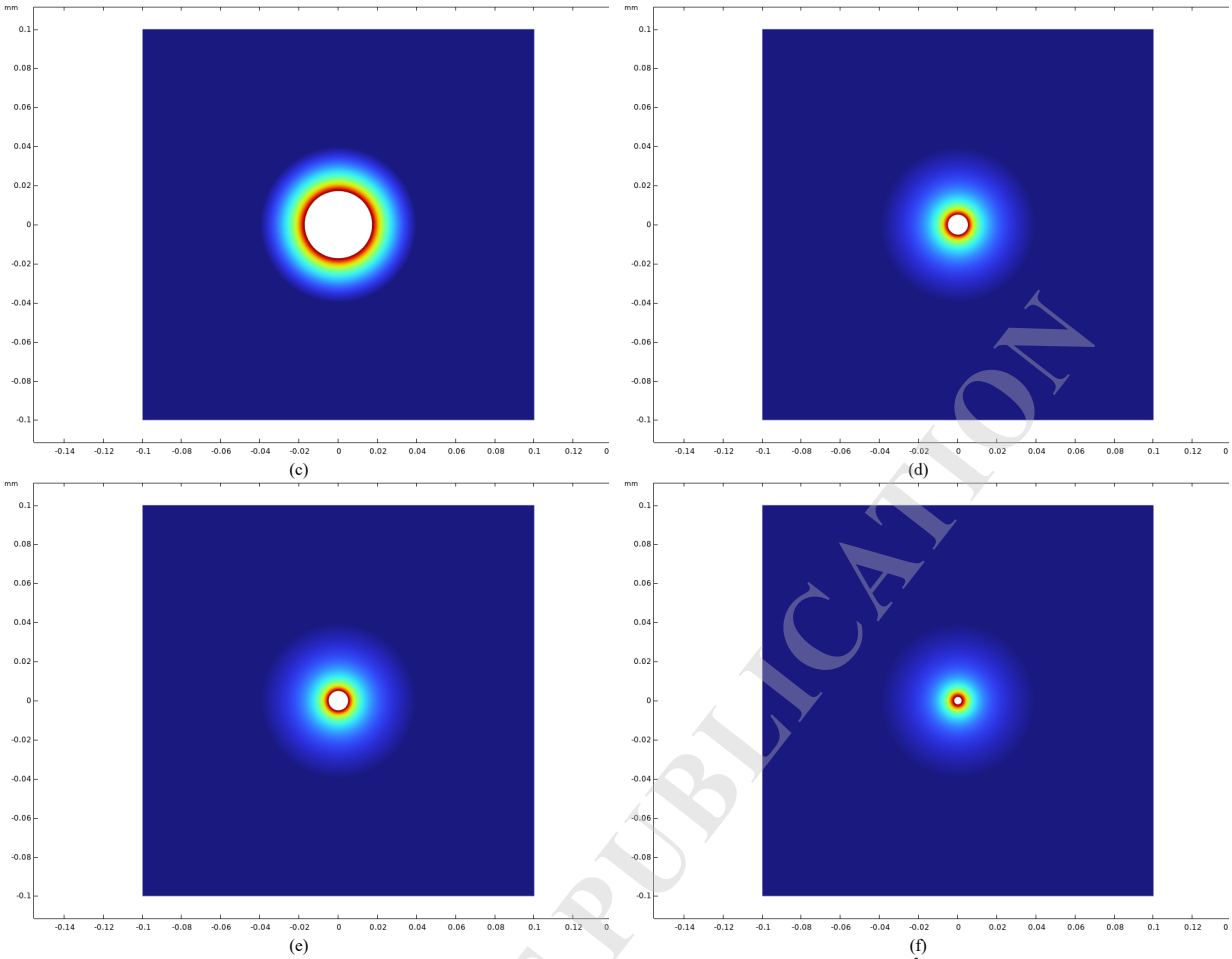

Figure 6 Cloud images of bubble maximum expansion and minimum contraction at different frequencies. (R_0=5 μm, P_d=1.32×10^5 Pa).(a)-(c) Maximum expansion states at f=45 kHz, 80 kHz, and 100 kHz; (d)-(f) Minimum contraction states at the corresponding frequencies.

Specifically, the dynamic evolution of a bubble with an initial radius of 5 μm in an acoustic oscillation cycle is simulated. Figure 6 (a), (b), and (c) shows the deformation of the bubble when it expands to its maximum under the action of the acoustic field with frequencies of 45 kHz, 80 kHz and 100 kHz, respectively. Correspondingly, Figure 6 (d), (e), and (f) depict the deformation of the bubble when it shrinks to its minimum under the excitation of the above acoustic field frequencies.

The result indicates that the bubble exhibits complex nonlinear oscillations within an acoustic cycle. During this process, the bubble first expands to its maximum volume during the negative pressure phase, followed by a rapid contraction to its minimum size under the subsequent positive pressure phase. This oscillatory behavior persists until eventual bubble collapse occurs. Furthermore, it is observed that lower acoustic frequencies lead to larger bubble oscillations and stronger nonlinear effects.

The bubble exhibits nonlinear oscillation under a certain acoustic field excitation, and the oscillation of its radius with time is shown in Figure 7.

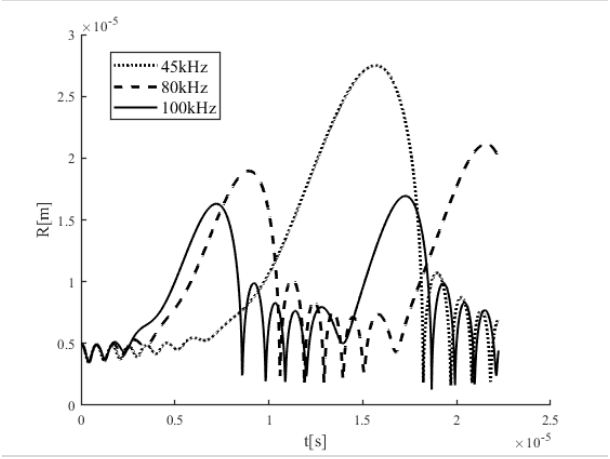

Figure 7 Response curve of the bubble radius with time(R_0=5 μm, P_d=1.32×10^5 Pa)

The result indicates that the oscillation amplitude of the bubble under the action of the acoustic field with a frequency of 45 kHz is much greater than that of the bubble under the action of the acoustic field with a frequency of 80 kHz and 100 kHz. The greater the oscillation amplitude of the bubble, the more intense the nonlinear oscillation of the bubble becomes, and consequently, the higher the energy accumulated within the bubble.

The results confirm that under the action of the acoustic field with a frequency of 45 kHz, the nonlinear oscillation of the bubble in Rh B solution is most pronounced, as well as the degradation efficiency of the solution is the best. That is to say, the simulation result is consistent with the experimental result, and the degradation rate of Rh B is closely related to the intensity of the nonlinear oscillation of the bubbles.

4.2. Numerical simulation of acoustic response of a bubble in Rh B solution

The extremely high temperature generated within cavitation bubbles constitutes a key characteristic for investigating the cavitation effect of acoustic fields and plays a crucial role in elucidating the physical mechanisms underlying ultrasonic degradation of organic pollutants.

Figure 8 shows that the maximum temperature inside the bubble increases with the increasing amplitude of the acoustic pressure. Specifically, when the driving frequency of the acoustic field is 45 kHz and the acoustic pressure amplitude reaches 1.46×10^5 Pa, the maximum temperature inside the bubble will reach a value of 6773 K.

The research results demonstrate that under the action of a low frequency acoustic field, the larger the amplitude of the acoustic pressure, the greater the radial pulsation amplitude of the bubble, and the more intense of its nonlinear oscillations. Thus, it is easier to accumulate energy within the bubble, creating extremely high temperature conditions and triggering intense cavitation effects.

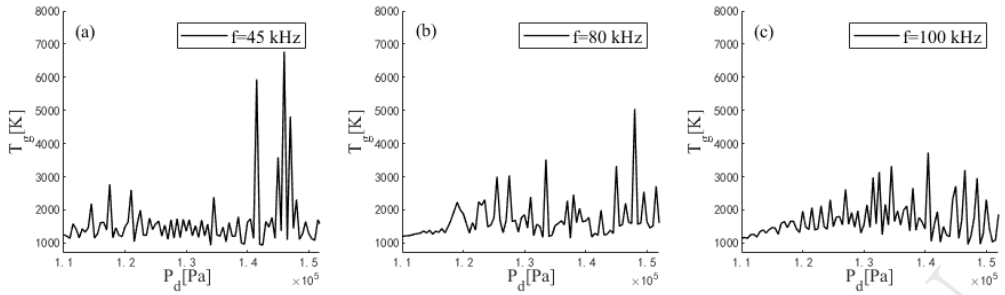

Figure 8 Response curve of the maximum temperature inside the bubble with the amplitude of acoustic pressure(R_0=5 μm).

The initial radius of the bubble has a significant impact on the acoustic response of the bubble in the acoustic field. As shown in Figure 9, the maximum temperature of a bubble initially increases with the initial radius, followed by a gradual and steady decrease. Under a driving acoustic field with a frequency of 45 kHz and pressure amplitude of 1.32×10^5 Pa, the maximum temperature reaches 4934 K when R_0 equals 6.2 μm. When R_0 is less than 32 μm, the maximum temperature inside the bubble exhibits a sharp nonlinear growth characteristic with the R_0 response curve. However, while R_0 is greater than 32 μm, the temperature becomes more stable and shows a consistent decline as R_0 increases.

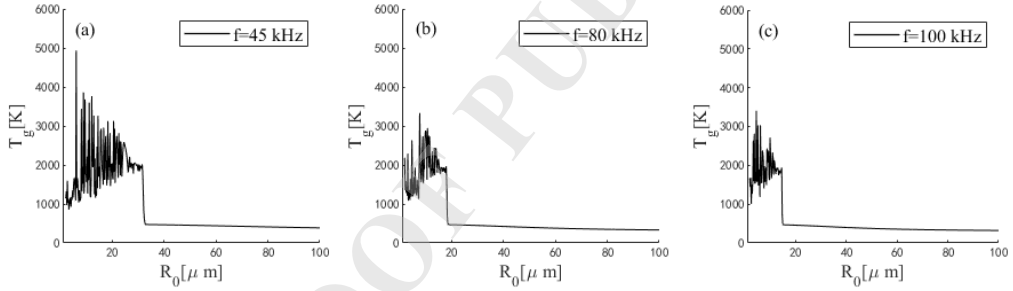

Figure 9 Response curve of maximum temperature inside the bubble with the initial radius of bubbles (P_d=1.32×10^5 Pa).

The numerical simulation results indicate that higher driving frequency of the acoustic field leads to weaker nonlinear oscillations of the bubble, reduces the energy accumulation, and consequently reduces the temperature within the bubble. Furthermore, the range of bubble radii inducing cavitation effects diminishes significantly with the increasing of the driving frequency. It suggests that smaller bubbles are more prone to generating intense cavitation effects under low frequency acoustic fields, which may offer extreme conditions of high temperature which are suitable for the ultrasonic degradation processes.

Under the influence of the acoustic field, the variation of the pressure inside the bubble is a key characteristic for investigating the acoustic cavitation effect, and it is theoretical foundation for the ultrasonic degradation of organic pollutants. The amplitude of the acoustic pressure determines the magnitude of the external force acting on the bubble.

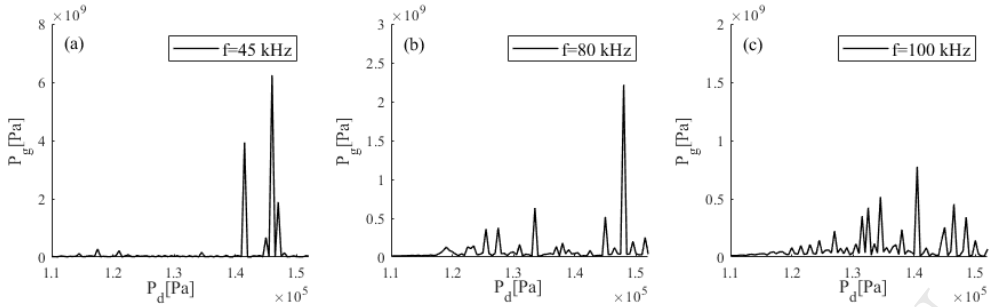

Figure 10 Response curve of maximum pressure inside the bubble with the amplitude of acoustic pressure (R_0=5 μm).

Figure 10 shows the response curves of the maximum pressure of a bubble in Rh B solution under the driving acoustic fields. When the bubble is subjected to an acoustic field with a frequency of 45 kHz and an acoustic pressure amplitude of 1.46×10^5 Pa, the maximum pressure reaches 6.24×10^5 Pa.

The result indicates that higher acoustic pressure amplitude leads to greater bubble expansion during the negative pressure phase, resulting in an increase of the kinetic energy during the compression phase and more intense nonlinear oscillations. Under low frequency acoustic field excitation, larger intense bubble oscillations are more likely to generate extreme pressure inside the bubble. Therefore, it may create a favorable condition for the chemical reactions that facilitate the degradation of organic pollutants.

Figure 11 shows the response curves of the maximum pressure of a bubble in Rh B solution with the initial bubble radius.

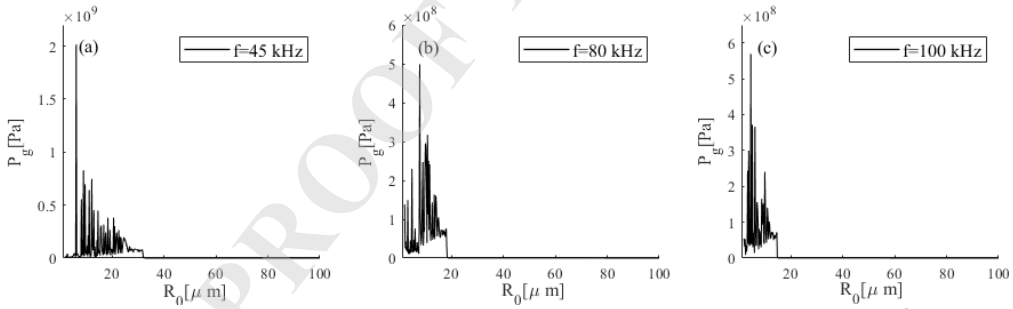

Figure 11 Response curve of maximum pressure inside the bubble with with the initial radius of bubbles (P_d=1.32×10^5 Pa).

As shown in the Figure 11, under a certain excitation of an acoustic field, the maximum pressure inside the bubble with the R_0 response curve shows the characteristics of first nonlinear growth and then stable change. When the driving frequency of the acoustic field is 45 kHz, the most intense nonlinear oscillation occurs when R_0 is less than 32 μm.

The results indicate that high frequency acoustic fields tend to suppress the oscillation of larger bubbles, whereas the small bubbles exhibit strong nonlinear oscillations under low frequency acoustic fields. The higher the pressure in the bubble, the stronger the cavitation effect may be generated.

Under the excitation of the acoustic field, the expansion-contraction ratio of the bubble serves as a crucial parameter, which reflects their energy conversion capability during oscillation (Wang C. *et al*.,

2017). Figure 12 presents the variation curves of bubble expansion-contraction ratio with the acoustic pressure amplitude in Rh B solution.

It can be observed from Figure 12 that the bubble expansion-contraction ratio increases with the increasing amplitude of the acoustic pressure. Under the influence of the acoustic field with a frequency of 45 kHz and an acoustic pressure amplitude of 1.46×10^5Pa, the bubble expansion-contraction ratio reaches its maximum value of 96.

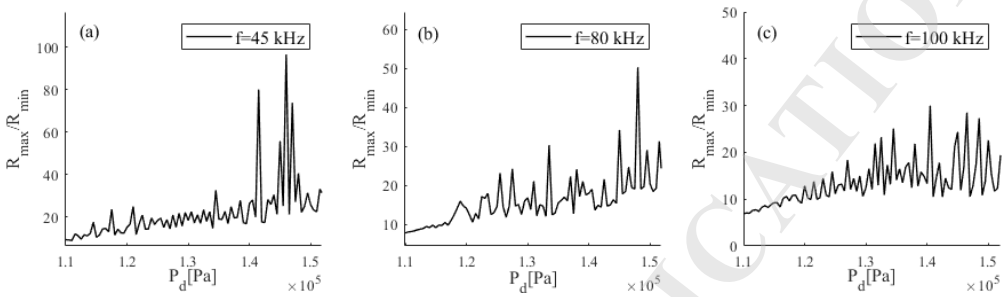

Figure 12 Response curve of the bubble expansion/contraction ratio with the amplitude of acoustic pressure (R_0=5 μm).

The research findings show that a lower acoustic field frequency and a higher acoustic pressure amplitude result in a greater bubble expansion-contraction ratio. During the nonlinear oscillation process, the bubble is more capable of accumulating acoustic energy, exhibit higher energy conversion efficiency, and is more likely to generate a pronounced acoustic response. In contrast, under the high frequency acoustic fields, the nonlinear oscillation behavior of the bubble weakens, resulting in a smaller expansion-contraction ratio and reduced energy conversion efficiency.

Figure 13 presents the response curves of the bubble expansion-contraction ratio in Rh B solution with the initial bubble radius under the influence of the acoustic fields. As shown in the Figure 13, while the driving frequency of the acoustic field is 45 kHz, the bubble expansion-contraction ratio with the R_0 response curve exhibits significant nonlinear downward trend when the initial radius is less than 32 μm. When R_0 exceeds 32 μm, the curve gradually declines and eventually stabilizes as R_0 increases.

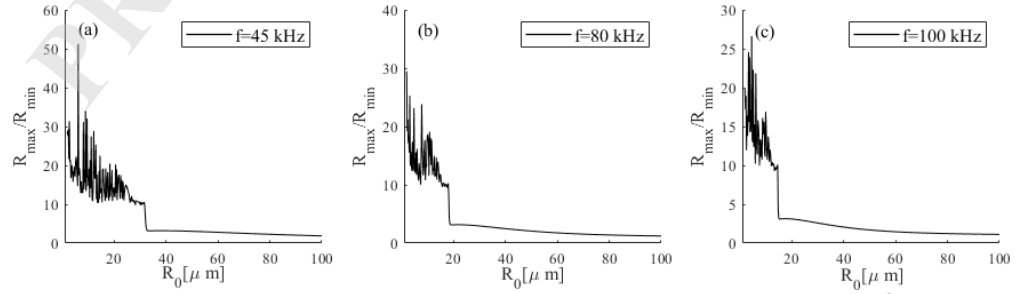

Figure 13 Response curve of the bubble expansion/contraction ratio with the initial radius of bubble(P_d=1.32×10^5 Pa).

The result indicates that smaller bubbles experience pronounced nonlinear oscillations under low frequency acoustic fields, leading to high energy conversion efficiency within the bubble. This

phenomenon maybe creates favorable conditions for chemical reactions, thereby enhancing the ultrasonic degradation of the organic compounds.

Under the actuation of the acoustic fields, the extremely high temperature and high pressure inside the cavitation bubble occurs with the associated shock wave generation. In the recent book (Chen, 2014) it was suggested that when the Mach number in the bubble is greater than 1, the shock wave will occur, and the size of the Mach number in the bubble is another important indication of the strong acoustic effect of the liquid around the bubble.

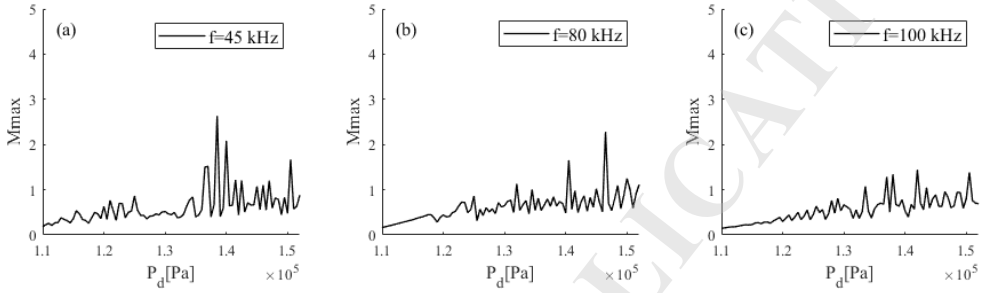

Figure 14 Response curve of the maximum Mach number inside the bubble with the amplitude of acoustic pressure (R_0=5 μm).

Figure 14 presents the response curves of the maximum Mach number of a bubble in the Rh B solution with the amplitude of the acoustic pressure. The figures show that the maximum Mach number increases nonlinearly with the increasing amplitude of the acoustic pressure. The greater the driving amplitude, the more intense the nonlinear oscillation of the bubble, and the higher the Mach number value.

The results show that the lower the acoustic field driving frequency and the greater the amplitude, the more violent the nonlinear oscillation of the bubble will be, and the higher the energy accumulated inside the bubble, as well as the more powerful the shock wave may be generated when the bubbles collapses.

Figure 15 shows that under the action of the acoustic field with a frequency of 45 kHz, the maximum Mach number inside the bubble with the R_0 response curve exhibits strong nonlinear growth while R_0<32 μm. The higher the driving frequency of the acoustic field, the weaker the nonlinear oscillation amplitude of the bubble, and the smaller the corresponding Mach number value.

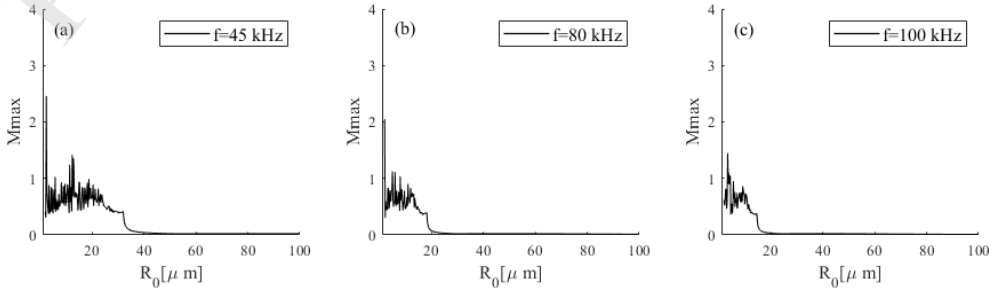

Figure 15 Response curve of the maximum Mach number inside the bubble with the initial radius of bubble (P_d=1.32×10^5 Pa).

The results show that small bubbles exhibit nonlinear oscillations driven by the low frequency acoustic field and may generate strong shock waves. As the driving frequency increases, the range of the bubble radius that may induce intense acoustic effects significantly shrinks. This suggests that high frequency acoustic field has an inhibitory effect on the nonlinear oscillation of bubbles.

5. Discussion

5.1. Correlation between Experiments and Simulations

The experimental results indicate that the degradation efficiency reaches its maximum at an ultrasonic driving frequency of 45 kHz. Theoretical simulations corroborate that the cavitation effect is most pronounced at this frequency, showing a high degree of consistency between experimental observations and simulation data.

The results show that under the driving of a certain acoustic field, the bubble vibrates nonlinear oscillations, which form an extremely high temperature and high-pressure environment in the bubble and shock waves. The lower the driving frequency of the acoustic field, the larger the acoustic pressure amplitude. The smaller the bubble size is, the more intense the nonlinear oscillation of the bubble is. The larger the value of internal temperature, pressure and Mach number, the higher the energy conversion efficiency will be. These extreme conditions may cause the decomposition of water vapor inside the bubbles into H • and OH • radicals, creating intense local mechanical effects, such as microjects and shear forces. The synergistic interaction between mechanical forces and chemical reactions during bubble collapse is strengthened, significantly promoting the degradation of Rh B.

5.2. Resolving Discrepancies

The result indicate that at a constant acoustic frequency of 45 kHz, the measured average acoustic intensity is highest at an acoustic power of 180 W, followed by 240 W, and lowest at 120 W(Table 1). In contrast, the degradation rate of the solution under the same frequency exhibits a different order: it is maximum at 180 W, followed by 120 W, and minimum at 240 W.(Figure 5) This discrepancy arises because the experimentally measured intensity represents a spatial average, which is predominantly influenced by the excitation frequency and power. However, the actual degradation efficiency is not solely determined by the overall acoustic intensity; it also critically depends on the localized extreme temperatures, high pressures, and concentrations of free radicals generated during cavitation bubble collapse. At an acoustic power of 240 W, although the average acoustic intensity is higher than that at 120 W, the excessive number of cavitation bubbles formed leads to significant acoustic scattering and energy dissipation. This "shielding

effect" reduces the effective energy transferred to individual collapsing bubbles, thereby diminishing the overall degradation efficiency. Furthermore, the local acoustic intensity at bubble nucleation sites, which governs the degradation process, may not scale linearly with the generator's power.

5.3. Novelty and Mechanistic Explanation

While bubble dynamics models are well-established, the novelty of this study lies in systematically establishing a quantitative correlation between macroscopic degradation experiments and microscopic bubble dynamics simulations. We not only validated the empirical observation that lower frequencies are more prone to inducing cavitation but also quantified the dynamic and acoustic response characteristics of bubbles under various acoustic fields, directly linking these microscopic physical quantities to macroscopic degradation performance. This integrated approach transcends the limitations of phenomenological descriptions, providing a concrete physical picture and a theoretical foundation for the targeted optimization of ultrasonic degradation processes. The key insight is that optimization efforts should focus on maximizing bubble oscillation amplitude and collapse intensity, rather than merely increasing ultrasonic power or decreasing the acoustic frequency.

5.4. Mechanistic Explanation of Transient Extreme Conditions

Numerical simulation results indicate that under a certain acoustic field excitation, the transient temperature inside cavitation bubbles can reach 5000 K, with pressures even attaining the order of 10^9 Pa. However, the duration of such extreme conditions is only on the order of microseconds or even shorter. Although this extremely brief timescale is insufficient to sustain large-scale or continuous chemical reactions, it is adequate to initiate the following critical processes: (1) pyrolysis of water vapor inside the bubbles, generating highly reactive free radicals, along with the direct pyrolysis of volatile pollutant molecules entrapped within the bubbles; and (2) generation of intense mechanical effects in the liquid surrounding the bubbles, such as shock waves and microjets. These mechanical effects not only directly induce shear cleavage of macromolecules but also significantly enhance liquid-phase mass transfer. Consequently, they act synergistically with radical oxidation reactions to promote the degradation of pollutants.

6. Conclusion

Under the acoustic field excitation, when the cavitation bubble is compressed to their minimum radius, it may generate extremely high temperature and high-pressure conditions which are unattainable in macroscopic systems. Simultaneously, the nonlinear oscillation and collapse of the cavitation bubble may

generate strong acoustic effects in the surrounding liquid, including acoustic microstreaming, liquid jetting, and shock waves. These phenomena may create favorable conditions for ultrasonic degradation of organic pollutants.

In this study, the cavitation activity under varying acoustic field parameters is quantitatively assessed through iodometric monitoring of I_3^- formation in ultrasonically irradiated potassium iodide solutions. The synergistic effects of acoustic field intensity, ultrasonic driving frequency, sonication time, and power on the degradation of Rh B are systematically investigated. Additionally, the dynamic evolution of a single spherical bubble under the influence of an ultrasonic field is simulated using Rh B solution as a model for the printing and dyeing wastewater. Combined with theoretical numerical analysis, we investigated the nonlinear oscillation of bubbles in Rh B solution under the ultrasonic irradiation. The internal energy conversion, temperature variation, pressure generation and shock wave formation, and other cavitation effects as well as their influencing factors inside the bubble are studied. Furthermore, the physical mechanism underlying the ultrasonic degradation of Rh B solution is explored.

The results indicate that the degradation efficiency reaches its maximum at an ultrasonic driving frequency of 45 kHz. The lower the driving frequency of the acoustic field, the larger the acoustic pressure amplitude. The smaller the bubble size is, the more intense the nonlinear oscillation of the bubble is. The larger the value of internal temperature, pressure and Mach number, the higher the energy conversion efficiency will be, which is more conducive to providing ideal reaction conditions for the ultrasonic degradation of organic pollutants.

Acoustic field intensity, which is influenced by both frequency and power, plays a key role in degradation efficiency.However it is not the sole determining factor, as nonlinear field effects can modulate the cavitation outcome. The high consistency between experimental observations and simulation data corroborates that the cavitation effect is most pronounced at this frequency, thereby establishing a clear mechanistic link: acoustic parameters→bubble dynamics→collapse energy→degradation efficiency. This mechanistic understanding, developed using Rh B as a model, provides a valuable framework for optimizing the ultrasonic degradation of a broader range of organic pollutants.

In future work, we plan to incorporate experimentally measured, frequency and power dependent acoustic intensities (as shown in Table 1) into the model to achieve a more quantitative agreement with the degradation experiments. Building on this, further investigations should extend to multi-bubble systems and their interactions, address more complex wastewater matrices, and employ in-situ diagnostic

techniques. These efforts will be crucial to further validate and refine the proposed mechanism for practical applications.

Declaration of Competing Interest

The authors declare that they have no known competing financial interests or personal relationships that could have appeared to influence the work reported in this paper.

Acknowledgements

This work was supported by the National Natural Science Foundation of China (Grant No. 12164037 and 62262054) and the Natural Science Foundation of Ningxia (Grant No. 2026AAC020113 and 2025AAC030585).

References

1 Alfonso-Muniozguren, P. et al. (2021), A review on pharmaceuticals removal from waters by s ingle and combined biological, membrane filtration and ultrasound systems, *Ultrasonics Sonochemist ry*, **76**(3): 105656, https://doi.org/10.1016/j.ultsonch.2021.105656.

2 Chen X., Dai J., Shi G., Li, L. Wang, G., Yang, H. (2016), Sonocatalytic degradation of Rho damine B catalyzed by β-Bi2O3 particles under ultrasonic irradiation, *Ultrasonics Sonochemistry*, **2 9**: 172-177, https://doi.org/10.1016/j.ultsonch.2015.08.010.

3 Chen, H. et al. (2024), Ultrasonic-driven degradation of organic pollutants using piezoelectric c atalysts WS2/Bi2WO6 heterojunction composites, *Chemosphere*, **364**: 143008, https://doi.org/10.1016/ j.chemosphere.2024.143008.

4 Chen, W. Z. (2014), *Acoustic cavitation physics*, [in Chinese: 声空化物理], Science Press, Bei jing, China.

5 Gogate P.R., Shirgaonkar I.Z., Sivakumar M. et al. (2001), Cavitation reactors: Efficiency asse ssment using a model reaction, *AIChE Journal*, **47**(11): 2526–2538, https://doi.org/10.1002/aic.690471 115.

6 Hao, O. J., Kim, H., & Chiang, P. C. (2000), Decolorization of Wastewater, *Critical Reviews i n Environmental Science and Technology*, **30**(4): 449–505, https://doi.org/10.1080/10643380091184237.

7 Holkar, C.R., Jadhav, A. J., Pinjari, D.V., Mahamuni, N.M., Pandit, A.B. (2016), A critical rev iew on textile wastewater treatments: possible approaches, *Journal of Environmental Management*, **1 82**: 351-366, https://doi.org/10.1016/j.jenvman.2016.07.090.

8 Kanthale, P., Ashokkumar, M., Grieser, F. (2008), Sonoluminescence, sonochemistry (H2O2 yield) and bubble dynamics: Frequency and power effects, *Ultrasonics Sonochemistry*, **15**(2): 143-150, https://doi.org/10.1016/j.ultsonch.2007.03.003.

9 Kashyap, N., Roy, K., Moholkar, V. S. (2020), Mechanistic investigations in ultrasound-assisted biodegradation of phenanthrene. *Ultrasonics Sonochemistry*, **62**(C): 104890 https://doi.org/10.1016/j.ultsonch.2019.104890.

10 Li W. (2023), Cavitation bubble behavior on nanodiamond surface and its mechanism on cyanobacterial rmoval, [in Chinese: 声场中空化泡在纳米金刚石表面的行为及其除藻机制的研究], Master Disseration, College of Environmental Science and Engineering, Yangzhou University.

11 Liu Z. C., Khan T.A., Islam M. A., Tabrez U. (2022), A review on the treatment of dyes in printing and dyeing wastewater by plant biomass carbon, *Bioresource technology*, **354**:127168, https://doi.org/10.1016/j.biortech.2022.127168.

12 Liu, S. et al. (2025), Recent advances in ultrasound-fenton/fenton-like technology for degradation of aqueous organic pollutants, *Chemosphere*, **352**: 141286, https://doi.org/10.1016/j.chemosphere.2024.141286.

13 Ma, Y., Shen X, Zhang N. (2012), The Research of Degradation of RhB with Dual-frequency Ultrasound, [in Chinese: 相向双频超声降解罗丹明 B(RhB)的实验研究], *Journal of Ningxia Teachers University*, **33**(06):40-43. https://doi.org/10.3969/j.issn.1674-1331.2012.06.009.

14 Merouani, S., Hamdaoui, O., Saoudi, F., Chiha, S. (2010), Sonochemical degradation of Rhodamine B in aqueous phase: Effects of additives, *Chemical Engineering Journal*, 158(3): 550-557. https://doi.org/10.1016/j.cej.2010.01.048.

15 Métayer L., Olivier, Saurel R. (2016), The Noble-Abel Stiffened-Gas equation of state, *Physics of fluids*, **28**(4): 1713-1741. https://doi.org/10.1063/1.4945981.

16 Sadeghi, M., Zarshenas, P. (2024), Ultrasound-assisted heterogeneous process for organic dye pollutants destruction using the novel MIL-101(Fe)/ZrO2/MnFe2O4 nanocomposite catalyst from water medium, *Journal of Environmental Health Science and Engineering*, **22**(2): 483-501, https://doi.org/10.1007/S40201-024-00906-0.

17 Tatake, P.A., Pandit A.B. (2002), Modelling and experimental investigation into cavity dynamics and cavitational yield: influence of dual frequency ultrasound sources, *Chemical Engineering Science*, **57**(22–23): 4987–4995, https://doi.org/10.1016/S0009-2509(02)00271-3.

18 Wang B., et al. (2024), Bubble dynamics model and its revelation of ultrasonic cavitation beh avior in advanced oxidation processes: A review, *Journal of Water Process Engineering*, **63**. https://doi.org/10.1016/j.jwpe.2024.105470.

19 Wang C., Mo R., Hu J., Zhang M. (2017), Vibration characteristic of bubbles inside a spheric al cluster, [in Chinese: 泡群内气泡振动特性分析] *SCIENTIA SINICA Physica, Mechanica & Astron omica*, **47**(02):59-67. https://doi.org/10.1360/SSPMA2016-00316.

20 Wei, H., et al. (2024), Degradation of Rhodamine B via piezoelectric photocatalyst Bi2WO6res ponding to visible light and ultrasound: performance and mechanism, *Water Air Soil* Pollution, **235** (9), https://doi.org/10.1007/s11270-024-07386-w.

21 Xu W., He Y., Wang Y. (2006), Study on the Iodine Release in Kl Solution Caused by Ultras onic Irradiation, [in Chinese: 超声作用下碘化钾溶液生成碘速率的影响因素研究], *Journal of Chem ical Engineering of Chinese Universities*, **20**(03):472-475. https://doi.org/10.3321/j.issn:1003-9015.200 6.03.028.